a

Retinal cell types labeled in Cre lines screened by crossing with reporter					
Table 1 #	**Line**	**GCL**	**RGCs**	**INL**	**Cell Classes**
2	Adcyap1-2A-Cre	+	no	+	AC, HC, MG
4	Calb2-IRES-Cre	++	yes	++	AC, HC
5	Cart-IRES2-Cre	++	yes	+	AC
7	Cck-IRES-Cre	+	yes	++	AC, BC, MG
8	Cdh4-CreER	+	yes	+	AC, HC
9	Cdh6-CreER	+	yes	+	AC, HC
11	Chrna2-Cre_OE25	-	no	++	AC
13	Cnnm2-Cre_KD18	+	yes	+	AC
20	Dcx-CreERT2	++	yes	++	AC, BC
	Dlx5-CreERT2	-	no	+	MG
28	Fezf1-2A-Cre	+	no	++	AC, BC
37	Gpr26-Cre_KO250	++	yes	+	AC
39	Grm2-Cre_MR90	++	no	++	AC
40	Grp-Cre_KH288	+	yes	-	
42	Htr2a-Cre_KM207	+	yes	+	AC, BC
43	Ins2-Cre	+	?	++	AC, BC, HC, MG
44	Jam2-Cre	++	yes	++	AC
45	Jam2-CreER	+	yes	-	AC
47	Kcng4-Cre	+	yes	++	AC, BC
51	Neto1-Cre	+	yes	+	AC, BC
	Nos1-CreERT2	+	yes	++	AC
55	Otof-Cre	*damaged*		+	AC, MG
58	Pcdh9-Cre_NP276	++	yes	++	AC, HC, MG
59	Pde1c-2A-Cre	-	no	++	MG
67	Pvalb-IRES-Cre	++	yes	++	AC
68	Satb2-Cre_MO23	++	yes	+	AC, BC, MG
71	Sdk2-CreER	+	yes	+	AC, BC
72	Slc17a6-IRES-Cre	++	yes	-	
73	Slc18a2-Cre_OZ14	++	yes	-	
78	Sst-Cre	-	no	+	AC, BC, MG
	Tac1-IRES2-Cre	+	yes	+	AC
81	Tac2-IRES2-Cre	+	no	-	
87	Vipr2-Cre_KE2	++	yes	++	AC, BC, HC, MG

+ = present , ++ = numerous. Abbreviations; amacrine cells, AC; bipolar cells, BC; horizontal cells, HC; Muller glia, MG

b

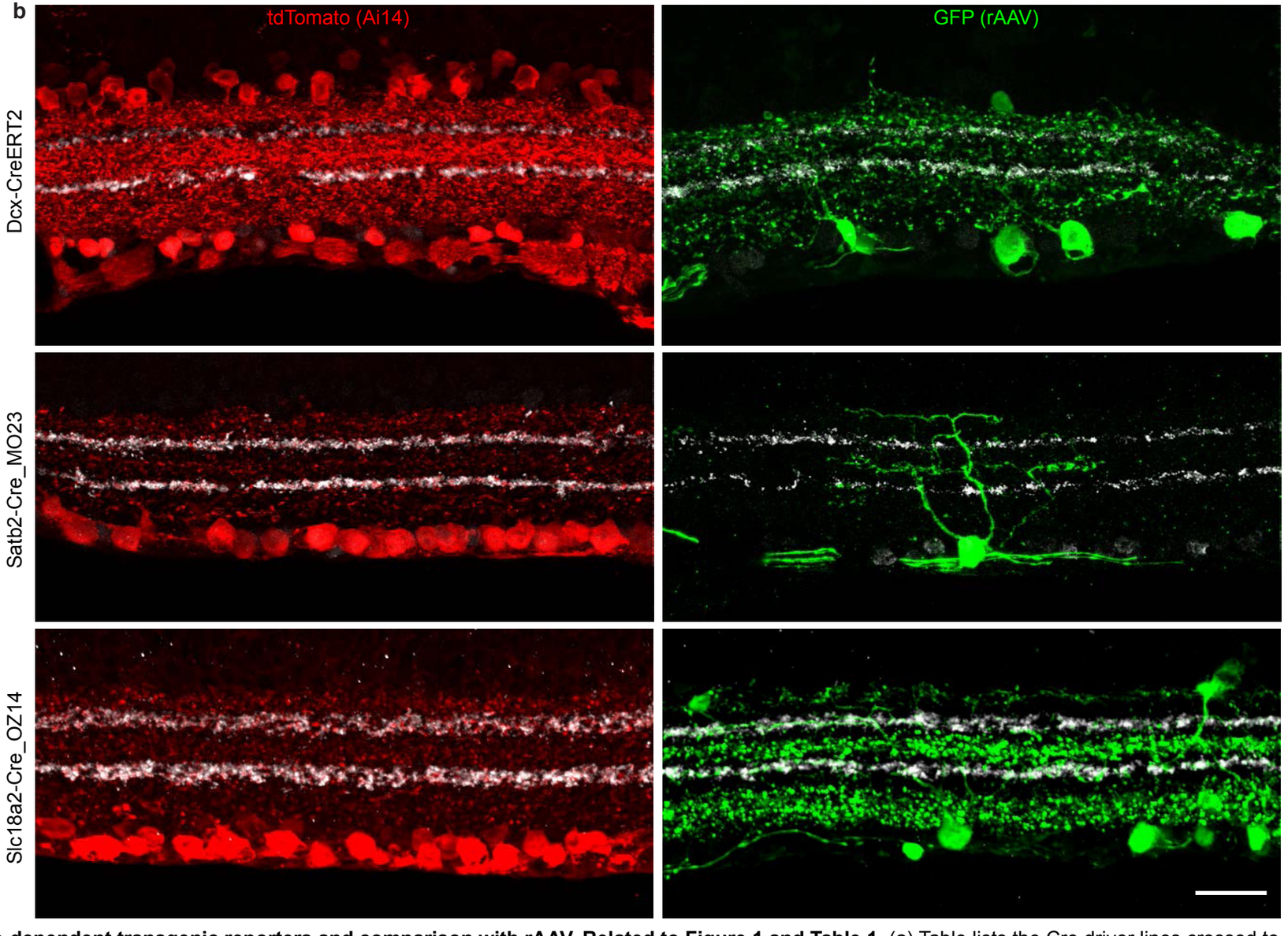

Figure S1. Retinal cell types labeled in Cre driver lines visualized by Cre-dependent transgenic reporters and comparison with rAAV, Related to Figure 1 and Table 1. (a) Table lists the Cre driver lines crossed to a Cre-dependent reporter line for visualizing transgene expression and the locations and classes of labeled cells. (b) Retinal images of reporter expression are shown for three Cre driver lines after crossing with the Ai14 reporter line (red) or following intravitreal injection of Cre-dependent rAAV reporter (green). Sections were also stained with anti-VAChT (white). In each case, the rAAV labels a subset of the cell types labeled by the Ai14 transgenic reporter. Scale bar 25μm.

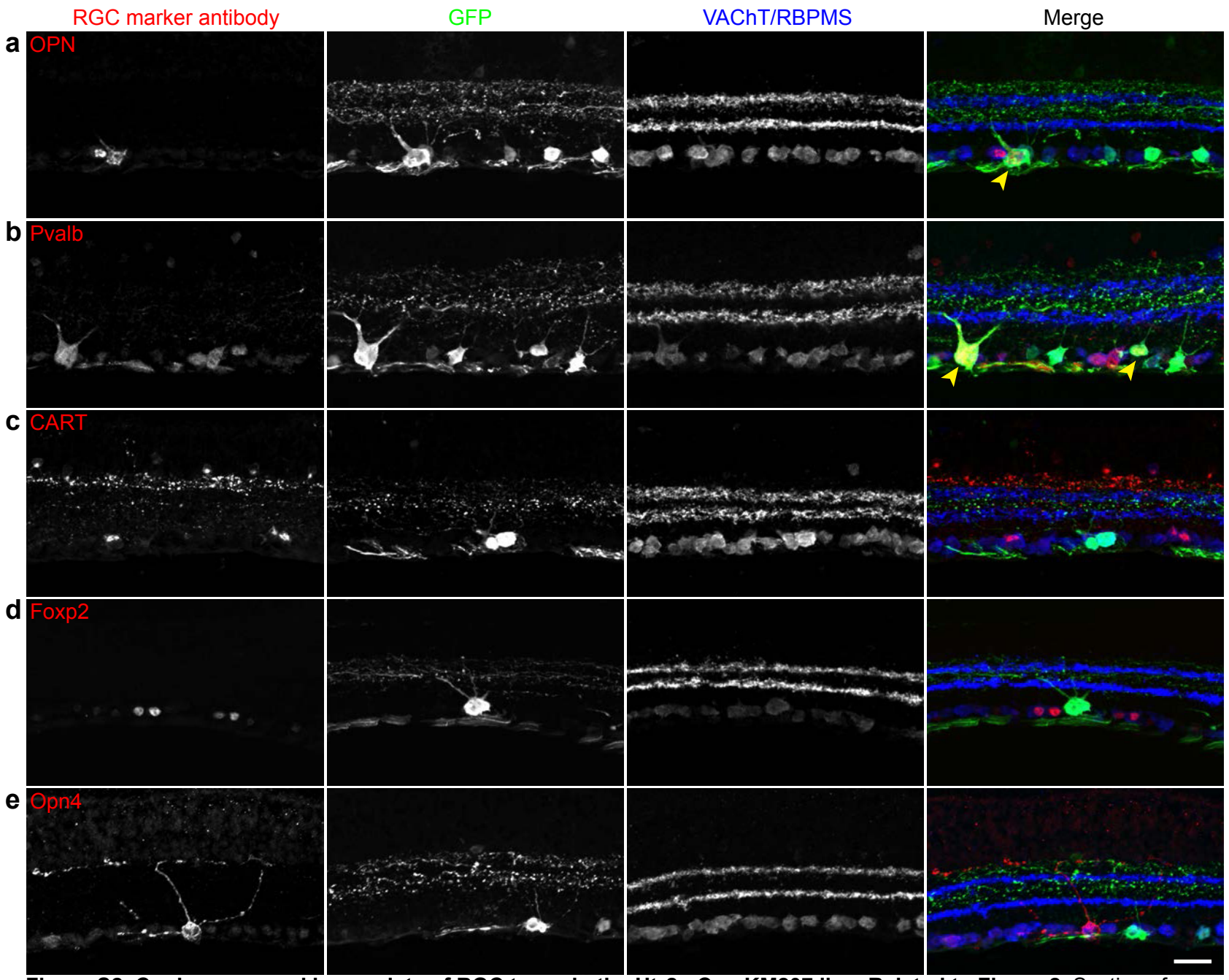

Figure S2. Cre is expressed in a variety of RGC types in the Htr2a-Cre_KM207 line, Related to Figure 2. Sections from an Htr2a-Cre_KM207 retina injected with Cre-dependent rAAV were stained with anti-GFP (green in merge), anti-VAChT, anti-RBPMS (both blue in merge), and other antibodies that mark specific RGC subtypes. (a) anti-osteopontin (OPN) labels alpha RGCs. (b) anti-parvalbumin (Pvalb) labels 8 RGC types including ooDSGCs and alpha RGCs. (c) anti-CART labels ooDSGCs. (d) anti-Foxp2 labels four F-RGC types. (e) anti-melanopsin (Opn4), labels ipRGC types M1 and M2. Scale bar 25μm.

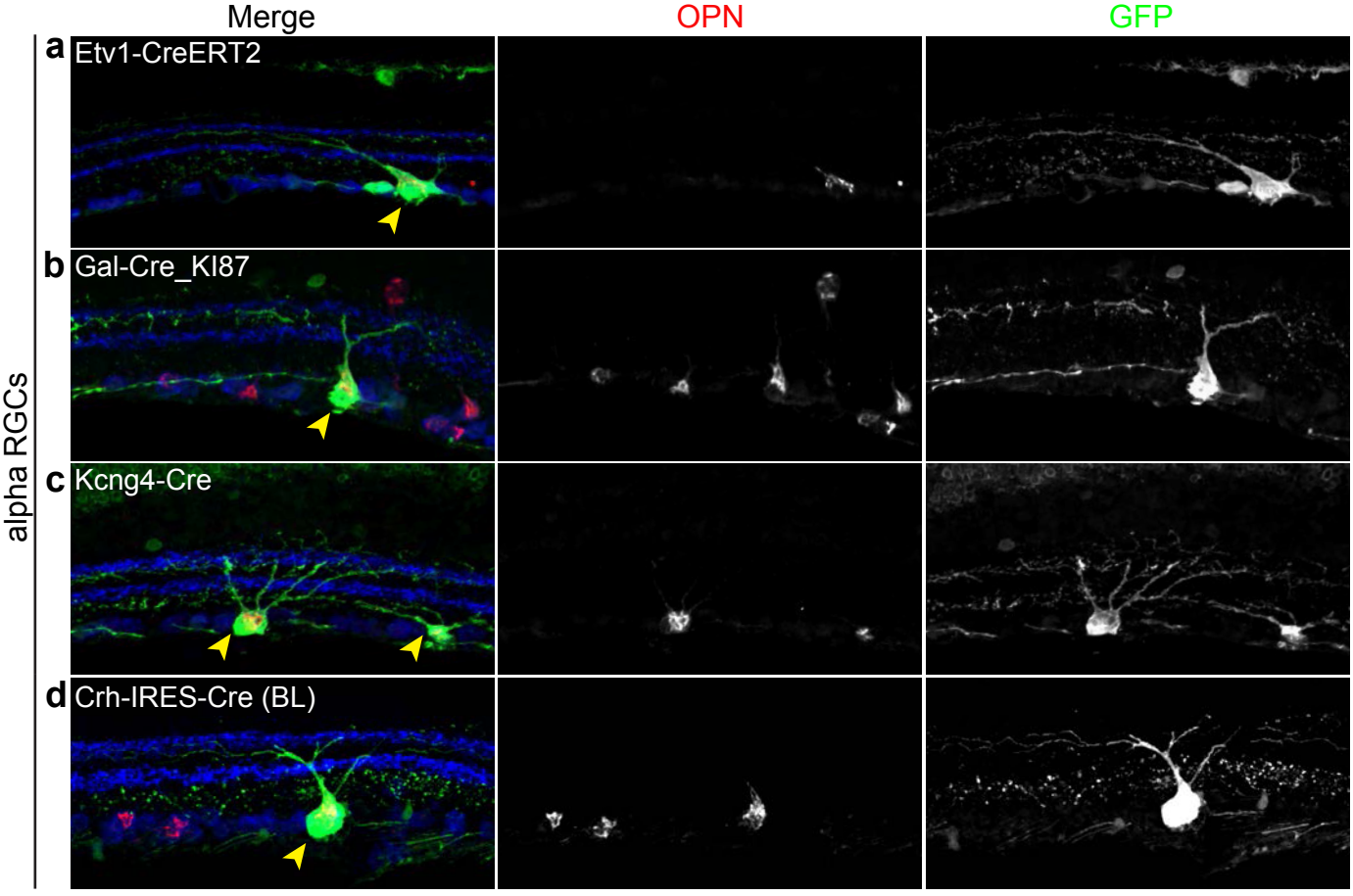

Figure S3. Cre lines that mark alpha RGCs, Related to Figures 1 and 2. (a-d) Vertical retina sections were stained with anti-GFP (green in merge), anti-VAChT and anti-RBPMS (both blue in merge), and (a-d) anti-OPN to label alpha RGCs (red in merge). Etv1-CreERT2 (a), Gal-Cre_KI87 (b), Kcng4-Cre (c), and Crh-IRES-Cre (BL) (d) selectively label osteopontin-positive alpha RGCs.

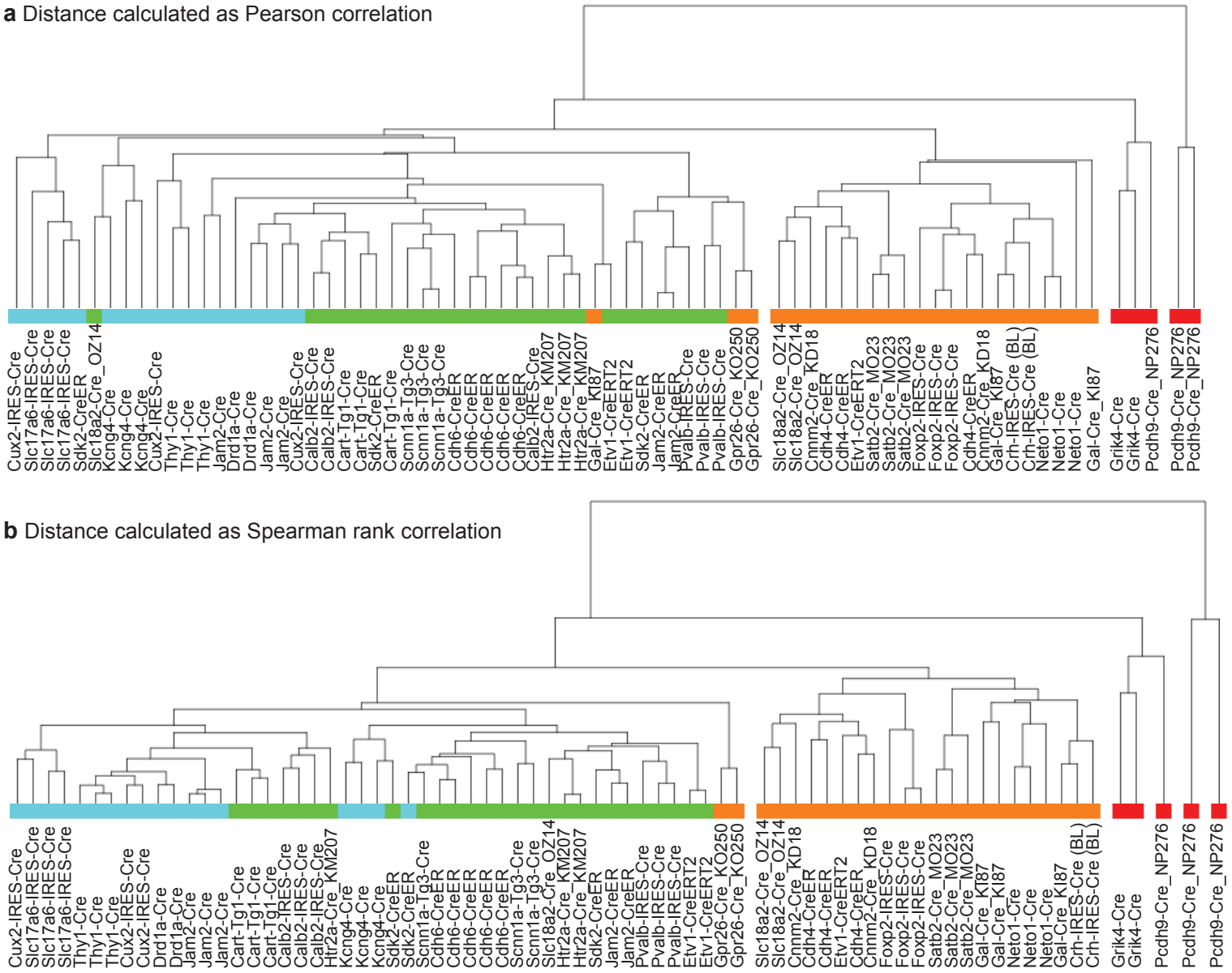

Figure S4. Alternative distance measures used to cluster individual experiments, Related to Figure 4. The resulting dendrograms are shown following unsupervised hierarchical clustering of the experiments using Pearson (a) and Spearman rank (b) correlation values as the distance measure. Cluster membership for each experiment was relatively stable across all distance measures used, although some experiments moved around (e.g. Gpr26-Cre lines are in the larger Cluster 1-2 in (a) and (b) as opposed to Cluster 3 in Figure 4. The colors indicate cluster assignment shown in Figure 4. Blue=Cluster 1, Green=Cluster 2, Orange=Cluster 3, Red=Cluster 4.

Table S1. Source and generation information for all Cre lines in Table 1.

Number	Line	GCL	RGCs	INL	Cell Classes	Generation Method	Type	Originating Lab (Donating Investigator)	Public Repository	Stock #
1	A930038C07Rik-Tg1-Cre	+	yes	+	AC, BC, MG	Transgenic	BAC	Allen Institute for Brain Science	The Jackson Laboratory	017346
2	Adcyap1-2A-Cre	++	yes	+	MG	Knock-in	T2A	Allen Institute for Brain Science	The Jackson Laboratory	007914
3	Agrp-IRES-Cre	+	yes	+	AC, BC, MG, PR	Knock-in	IRES	Brad Lowell	The Jackson Laboratory	012899
4	**Calb2-IRES-Cre**	**+**	**yes**	**+**	**AC, HC**	Knock-in	IRES	Z. Josh Huang	The Jackson Laboratory	010774
5	Cart-IRES2-Cre	+	yes	+	AC	Knock-in	IRES2	Allen Institute for Brain Science	The Jackson Laboratory	028533
6	**Cart-Tg1-Cre**	**++**	**yes**	**+**	**AC**	Transgenic	BAC	Allen Institute for Brain Science	The Jackson Laboratory	009615
7	Cck-IRES-Cre	+	yes	+	AC, BC	Knock-in	IRES	Z. Josh Huang	The Jackson Laboratory	012706
8	**Cdh4-CreER**	**+**	**yes**	**++**	**AC, HC**	Knock-in	Direct	Joshua Sanes		
9	**Cdh6-CreER**	**++**	**yes**	**+**	**AC**	Knock-in	Direct	Joshua Sanes		
10	Cdhr1-Cre_KG66	-	no	-		Transgenic	BAC	Nathaniel Heintz and Charles Gerfen	MMRRC	036056
11	Chrna2-Cre_OE25	-	no	-		Transgenic	BAC	Nathaniel Heintz and Charles Gerfen	MMRRC	036502
12	Chrnb4-Cre_OL57	+	yes	+	AC, HC, PR	Transgenic	BAC	Nathaniel Heintz and Charles Gerfen	MMRRC	036503
13	**Cnnm2-Cre_KD18**	**++**	**yes**	**+**	**AC**	Transgenic	BAC	Nathaniel Heintz and Charles Gerfen	MMRRC	030951
14	Cort-T2A-Cre	+	yes	++	AC, BC, HC	Knock-in	T2A	Z. Josh Huang	The Jackson Laboratory	010910
15	Crh-IRES-Cre (ZJH)	+	yes	+	AC	Knock-in	IRES	Z. Josh Huang	The Jackson Laboratory	012704
16	**Crh-IRES-Cre (BL)**	**+**	**yes**	**+**	**AC**	Knock-in	IRES	Brad Lowell		
17	**Cux2-IRES-Cre**	**++**	**yes**	**++**	**AC, BC, HC, MG**	Knock-in	IRES	Ulrich Mueller	MMRRC	031778
18	Dbh-Cre_KH212	-	no	-		Transgenic	BAC	Nathaniel Heintz and Charles Gerfen	MMRRC	032081
19	Dbx1-IRES-Cre	+	?	++	AC, HC, MG, PR	Knock-in	IRES	Ulrich Mueller	MMRRC	031751
20	Dcx-CreERT2	+	no	+	AC	Transgenic	Conventional	Ulrich Mueller	MMRRC	032780
21	Dcx-Cre-35	++	yes	+	AC	Transgenic	Conventional	Ulrich Mueller	MMRRC	031752
22	**Drd1a-Cre**	**++**	**yes**	**++**	**AC, BC, HC**	Knock-in	Direct	Richard Palmiter		
23	Drd2-Cre_ER44	+	yes	++	AC, BC, HC	Transgenic	BAC	Nathaniel Heintz and Charles Gerfen	MMRRC	032108
24	Drd3-Cre_KI196	+	yes	+	AC	Transgenic	BAC	Nathaniel Heintz and Charles Gerfen	MMRRC	034610
25	Efr3a-Cre_NO108	-	no	-		Transgenic	BAC	Nathaniel Heintz and Charles Gerfen	MMRRC	036660
26	Erbb4-2A-CreERT2	-	no	+	AC	Knock-in	F2A	Allen Institute for Brain Science	The Jackson Laboratory	012360
27	**Etv1-CreERT2**	**+**	**yes**	**+**	**AC**	Knock-in	Direct	Z. Josh Huang	The Jackson Laboratory	013048
28	Fezf1-2A-Cre	+	no	+	AC	Knock-in	T2A	Allen Institute for Brain Science		
29	**Foxp2-IRES-Cre**	**+**	**yes**	**+**	**AC**	Knock-in	IRES	Richard Palmiter		
30	Fstl4-CreERT2 / KIAA-CreER	+	yes	+	AC	Transgenic	BAC	Joshua Sanes		
31	Gabra6-IRES-Cre	++	yes	+	AC, BC	Knock-in	IRES	William Wisden	MMRRC	015968
32	Gabrr3-Cre_KC112	+	yes	++	BC, HC	Transgenic	BAC	Nathaniel Heintz and Charles Gerfen	MMRRC	030709
33	Gad2-IRES-Cre	+	?	++	AC	Knock-in	IRES	Z. Josh Huang	The Jackson Laboratory	010802
34	**Gal-Cre_KI87**	**+**	**yes**	**+**	**AC, PR**	Transgenic	BAC	Nathaniel Heintz and Charles Gerfen	MMRRC	031060
35	Gnb4-2A-Cre	+	yes	+	AC	Knock-in	T2A	Allen Institute for Brain Science		
36	Gng7-Cre_KH71	+	yes	+	AC	Transgenic	BAC	Nathaniel Heintz and Charles Gerfen	MMRRC	031181
37	**Gpr26-Cre_KO250**	**+**	**yes**	**+**	**AC**	Transgenic	BAC	Nathaniel Heintz and Charles Gerfen	MMRRC	033032
38	**Grik4-Cre**	**+**	**yes**	**+**	**AC**	Transgenic	BAC	Susumu Tonegawa	The Jackson Laboratory	006474
39	Grm2-Cre_MR90	+	yes	+	AC	Transgenic	BAC	Nathaniel Heintz and Charles Gerfen	MMRRC	034611
40	Grp-Cre_KH288	+	yes	+	AC, HC	Transgenic	BAC	Nathaniel Heintz and Charles Gerfen	MMRRC	031183
41	Hdc-Cre_IM1	-	no	+	AC, MG	Transgenic	BAC	Nathaniel Heintz and Charles Gerfen	MMRRC	032079
42	**Htr2a-Cre_KM207**	**+**	**yes**	**++**	**AC, BC**	Transgenic	BAC	Nathaniel Heintz and Charles Gerfen	MMRRC	031150
43	Ins2-Cre	+	yes	++	AC, BC, HC, MG	Transgenic	Conventional	Mark Magnuson	The Jackson Laboratory	003573
44	**Jam2-Cre**	**++**	**yes**	**++**	**AC**	Knock-in	Direct	Joshua Sanes		
45	**Jam2-CreER**	**+**	**yes**	**+**	**AC**	Transgenic	BAC	Joshua Sanes		
46	Kcnc2-Cre	-	no	+	AC, HC	Transgenic	Conventional	Susumu Tonegawa	The Jackson Laboratory	008582
47	**Kcng4-Cre**	**++**	**yes**	**+**	**BC**	Knock-in	Direct	Joshua Sanes		
48	Kiss1-Cre	+	yes	++	AC	Transgenic	BAC	Carol Elias		
49	Lepr-IRES-Cre	-	no	+	AC	Knock-in	IRES	Jeffrey Friedman	The Jackson Laboratory	008320
50	Gnrh1-Cre / Lhrh-Cre	-	no	-		Transgenic	BAC	Catherine Dulac		
51	**Neto1-Cre**	**+**	**yes**	**+**	**AC**	Knock-in	Direct	Joshua Sanes		
52	Nr5a1-Cre	-	no	-		Transgenic	BAC	Brad Lowell	The Jackson Laboratory	006364
53	Ntrk1-IRES-Cre	-	no	-		Knock-in	IRES	Louis F Reichardt	MMRRC	015500
54	Ntsr1-Cre_GN220	+	yes	+	AC, BC, HC, MG	Transgenic	BAC	Nathaniel Heintz and Charles Gerfen	MMRRC	030648
55	Otof-Cre	+	yes	+	BC, MG, PR	Knock-in	Direct	Ulrich Mueller	MMRRC	032781
56	Otof-CreERT2	-	no	-		Knock-in	Direct	Ulrich Mueller	MMRRC	032782
57	Oxt-IRES-Cre	-	no	+	AC, BC, HC	Knock-in	IRES	Brad Lowell		
58	**Pcdh9-Cre_NP276**	**+**	**yes**	**+**	**AC**	Transgenic	BAC	Nathaniel Heintz and Charles Gerfen	MMRRC	036084
59	Pde1c-2A-Cre	+	yes	+	BC, MG	Knock-in	2A	Allen Institute for Brain Science		
60	Pdzk1ip1-Cre_KD31	+	yes	+	AC, BC, MG	Transgenic	BAC	Nathaniel Heintz and Charles Gerfen	MMRRC	030851
61	Pmch-Cre	+	yes	+	AC, BC, HC, MG, PR	Transgenic	BAC	Brad Lowell	The Jackson Laboratory	014099
62	Pnmt-Cre	-	no	+	AC	Knock-in	Direct	Steven Ebert		
63	Pomc-Cre (ST)	+	yes	++	AC	Transgenic	BAC	Susumu Tonegawa	The Jackson Laboratory	010714
64	Pomc-Cre (BL)	-	no	-		Transgenic	Conventional	Brad Lowell	The Jackson Laboratory	005965
65	Ppp1r17-Cre_NL146	+	yes	+	AC	Transgenic	BAC	Nathaniel Heintz and Charles Gerfen	MMRRC	036205
66	Prkcd-GluCla-CFP-IRES-Cre	+	yes	++	AC, BC, MG	Transgenic	BAC	David Anderson		
67	**Pvalb-IRES-Cre**	**++**	**yes**	**+**	**AC**	Knock-in	IRES	Silvia Arber	The Jackson Laboratory	008069
68	**Satb2-Cre_MO23**	**+**	**yes**	**+**	**AC, BC, HC**	Transgenic	BAC	Nathaniel Heintz and Charles Gerfen	MMRRC	032908
69	Scnn1a-Tg2-Cre	+	yes	+	AC	Transgenic	BAC	Allen Institute for Brain Science	The Jackson Laboratory	009112
70	**Scnn1a-Tg3-Cre**	**+**	**yes**	**+**	**AC**	Transgenic	BAC	Allen Institute for Brain Science	The Jackson Laboratory	009613
71	**Sdk2-CreER**	**+**	**yes**	**++**	**AC, HC**	Knock-in	Direct	Joshua Sanes		
72	**Slc17a6-IRES-Cre**	**++**	**yes**	**+**	**AC, HC**	Knock-in	IRES	Brad Lowell		
73	**Slc18a2-Cre_OZ14**	**+**	**yes**	**+**	**AC**	Transgenic	BAC	Nathaniel Heintz and Charles Gerfen	MMRRC	034814
74	Slc32a1-IRES-Cre	-	no	++	AC	Knock-in	IRES	Brad Lowell		
75	Slc6a3-Cre	-	no	+	AC	Knock-in	Direct	Xiaoxi Zhuang		
76	Slc6a4-Cre_ET33	+	yes	+	AC, HC, MG	Transgenic	BAC	Nathaniel Heintz and Charles Gerfen	MMRRC	031028
77	Slc6a5-Cre_KF109	-	no	+	AC	Transgenic	BAC	Nathaniel Heintz and Charles Gerfen	MMRRC	030730
78	Sst-Cre	-	no	-		Knock-in	Direct	Allen Institute for Brain Science		
79	Syt17-Cre_NO14	-	no	-		Transgenic	BAC	Nathaniel Heintz and Charles Gerfen	MMRRC	034355
80	Syt6-Cre_KI148	+	yes	-		Transgenic	BAC	Nathaniel Heintz and Charles Gerfen	MMRRC	032012
81	Tac2-IRES2-Cre	++	no	+	AC	Knock-in	IRES2	Allen Institute for Brain Science	The Jackson Laboratory	021878
82	**Thy1-Cre**	**++**	**yes**	**+**	**AC**	Transgenic	Conventional	Fred Van Leuven	The Jackson Laboratory	006143
83	Tlx3-Cre	-	no	-		Transgenic	BAC	Nathaniel Heintz and Charles Gerfen	MMRRC	036547
84	Trib2-2A-CreERT2	++	yes	++	AC, BC, MG	Knock-in	F2A	Allen Institute for Brain Science	The Jackson Laboratory	022865
85	Ucn3-Cre_KF43	-	no	+	AC, MG, PR	Transgenic	BAC	Nathaniel Heintz and Charles Gerfen	MMRRC	032078
86	Vip-IRES-Cre	-	no	++	AC	Knock-in	IRES	Z. Josh Huang	The Jackson Laboratory	010908
87	Vipr2-Cre_KE2	+	yes	++	AC	Transgenic	BAC	Nathaniel Heintz and Charles Gerfen	MMRRC	034281
88	Wfs1-Tg3-CreERT2	+	yes	+	AC	Transgenic	BAC	Allen Institute for Brain Science	The Jackson Laboratory	009103

+ = present , ++ = numerous. **BOLD** = line used for central projection mapping. Abbreviations; amacrine cells, AC; bipolar cells, BC; horizontal cells, HC; Muller glia, MG; photoreceptors, PR

Allen Mouse CCF Structure	CCF Name	Alternative Nomenclature or Assignment	Contra	Ipsi	Figure 5 Panel		Differences between Morin and Studholme (MS, 2014) and the current study
Hypothalamus							
Supraoptic nucleus	SO	SON/pSON	+	+	A,B,C,D,E		
Medial preoptic area	MPO	MPA	+**	-	A,B		
Subparaventricular zone	SBPV	sPa	+	+	D,E		
Suprachiasmatic nucleus	SCH	SCN	+	+	B,C,D		
Ventrolateral preoptic nucleus	VLPO		+***	-	not shown		Very sparse fibers (MS). None (current).
Anterior hypothalamic nucleus	AHN	AH/LA	+	+	B,C,D,E		
Lateral hypothalamic area	LHA	LH	+	+	C,D,E,F,G,H		
Lateral preoptic area	LPO	LPO/HDB	+	-	A,B		Very sparse fibers (MS). None (current).
Retrochiasmatic area	RCH		+	+	C,D,E		
Tuberal nucleus	TU	VMH	+**	+***	F		
Zona incerta	ZI		+	+	G,H,I		No fibers (MS). Fibers (current). Discrepancy may be due to difficulty in assigning LGv, PP, ZI.
Paraventricular hypothalamic nucleus	PVH	Pa	-	-			Very sparse fibers (MS). None (current).
Amygdala/Pallidum							
Anterior amygdalar area	AAA	AAv	+***	-	not shown		
Medial amygdalar nucleus	MEA		+	-	E,F,G		Sparse fibers (MS). None (current).
Substantia innominata	SI		+**	+**	F		No fibers (MS). Very sparse fibers (current).
Thalamus							
Peripeduncular nucleus	PP		+	+	J		
Medial geniculate complex	MG	DT	+	+	J,K		
Dorsal part of the lateral geniculate complex	LGd	DLG, LGN	+	+	G,H,I		
Lateral posterior nucleus of the thalamus	LP	lMA	+	+	G,H,I		
Suprageniculate nucleus	SGN	SG	+**	-	J		
Lateral dorsal nucleus of thalamus	LD		+	+**	F,G / F		Passing fibers (MS). Sparse terminals (current).
Central lateral nucleus of the thalamus	CL	PHb	+	-	F,G		
Intergeniculate leaflet of the lateral geniculate complex	IGL		+	+	H,I		
Ventral part of the lateral geniculate complex	LGv	VLG	+	+	G,H,I		
Subgeniculate nucleus	SubG		+	+	H		
Anterodorsal thalamus	AD	AD/BSTpm	-	-			Sparse fibers (MS). None (current). This location of BSTpm corresponds to AD in the CCF.
Midbrain							
Superior colliculus, sensory related	SCs	Zo,SuG,Op	+	+	J,K,L		
Medial terminal nucleus of the accessory optic tract	MT	tzSF	+	+	I,J		
Inferior colliculus	IC	DCIC	+*	-	not shown		
Superior colliculus, motor related	SCm	lnG	+	+	J,K,L		
Anterior pretectal nucleus	APN	APT/PLi	+	+	H,I,J		
Medial pretectal area	MPT		+	+***	H,I		
Nucleus of the optic tract	NOT		+	+	I,J		
Olivary pretectal nucleus	OP	OPT	+	+	H,I		
Posterior pretectal nucleus	PPT		+	+	I		
Lateral terminal nucleus of the accessory optic tract	LT		+	-	I		Sparse fibers (MS). None (current). Discrepancy may be due to difficulty in assigning LT and PP.
	none	CPT	-	-			Fibers (MS). None (current). Area not annotated in the CCF or Paxinos mouse atlas.
	none	PN	-	-			Very sparse fibers (MS). None (current). Area not annotated in the CCF.

Table S2. List of all retinorecipient regions identified after tracing the central projections of Thy1-Cre expressing retinal ganglion cells (n=3), Related to Figure 3. *excluded from quantitative analysis, very sparse labeling, but present in 3 of 3 Thy1-Cre mice, **excluded from quantitative analysis, very sparse labeling but in 2 of 3 Thy1-Cre mice, ***excluded from quantitative analysis, very sparse labeling and only present in 1 of 3 Thy1-Cre mice.

Fig. 4 RR Group	Fig. 4 Dendrogram Order	Table S2 Order	Major Region	Target	Kcng4-Cre	Etv1-CreERT2	Gal-Cre_KI87	Crh-IRES-Cre (BL)
1	1	13	Thalamus	LP-R	***	***	-	-
1	2	12	Thalamus	LGd-R	***	***	***	**
1	3	21	Midbrain	SCm-R	***	***	***	**
1	4	24	Midbrain	NOT-R	***	***	***	**
1	5	22	Midbrain	APN-R	***	***	***	**
1	6	19	Midbrain	SCs-R	***	***	***	**
1	7	25	Midbrain	OP-R	***	***	***	**
1	8	17	Thalamus	LGv-R	***	***	**	-
1	9	26	Midbrain	PPT-R	***	***	*	*
1	10	12	Thalamus	LGd-L	***	***	***	*
1	11	17	Thalamus	LGv-L	***	***	***	*
2	12	20	Midbrain	MT-R	-	-	-	-
2	13	11	Thalamus	MG-R	*	*	-	-
2	14	18	Thalamus	SubG-R	*	**	-	-
2	15	10	Thalamus	PP-R	***	**	-	-
2	16	8	Hypothalamus	ZI-R	***	-	-	-
2	17	18	Thalamus	SubG-L	**	*	**	-
2	18	10	Thalamus	PP-L	***	**	*	-
2	19	8	Hypothalamus	ZI-L	***	*	*	-
2	20	16	Thalamus	IGL-R	***	-	*	*
2	21	13	Thalamus	LP-L	***	**	*	-
2	22	16	Thalamus	IGL-L	***	**	**	*
2	23	25	Midbrain	OP-L	***	**	**	-
2	24	26	Midbrain	PPT-L	***	***	**	-
2	25	19	Midbrain	SCs-L	***	***	**	-
2	26	22	Midbrain	APN-L	***	**	*	-
2	27	24	Midbrain	NOT-L	***	***	*	-
2	28	21	Midbrain	SCm-L	***	**	-	-
3	29	7	Hypothalamus	RCH-L	***	-	-	-
3	30	7	Hypothalamus	RCH-R	***	-	-	-
3	31	3	Hypothalamus	SCH-L	***	-	*	-
3	32	3	Hypothalamus	SCH-R	*	-	-	-
3	33	11	Thalamus	MG-L	**	**	-	-
3	34	20	Midbrain	MT-L	-	-	-	-
3	35	27	Midbrain	LT-R	-	-	-	-
3	36	5	Hypothalamus	LHA-L	*	-	-	-
3	37	1	Hypothalamus	SO-L	*	-	-	-
3	38	4	Hypothalamus	AHN-L	**	-	-	-
3	39	2	Hypothalamus	SBPV-L	***	-	-	-
3	40	2	Hypothalamus	SBPV-R	***	-	-	-
3	41	4	Hypothalamus	AHN-R	**	-	-	-
3	42	6	Hypothalamus	LPO-R	**	-	-	-
3	43	15	Thalamus	CL-R	***	-	-	-
3	44	14	Thalamus	LD-R	**	-	-	-
3	45	5	Hypothalamus	LHA-R	***	-	-	-
3	46	1	Hypothalamus	SO-R	***	-	-	-
3	47	23	Midbrain	MPT-R	**	-	-	-
3	48	9	Amygdala	MEA-R	-	-	-	-

Table S3. Verified projections from four Cre lines enriched for alpha RGCs, Related to Figure 4. -; no projection, * terminals observed in n=1, ** n=2, *** n=3. Note that Crh-IRES-Cre (BL) had only n=2. The others had n=3.

Movie S1. Whole brain images of Thy1-Cre retinal ganglion cell axons, related to Figure 3. The movie shows the stack of 140 coronal plane images acquired every 100 μm using serial two-photon tomography. GFP-labeled axons from Thy1-Cre+ retinal ganglion cells can be seen entering the brain at the optic chiasm and radiating to many targets brain-wide, described in Figure 3.

Data S1. Log-transformed normalized projection values for each experiment and target, related to Figure 4. Projection strengths were measured as the sum of all algorithmically-detected fluorescent pixels within a given target region (projection volume), and normalized by the injection volume in the optic chiasm. These values were log-transformed and underlie the color map shown in Figure 4.

Supplemental Experimental Procedures

Transgenic mice

Mouse lines were maintained as heterozygotes by crossing with C57Bl6/J mice. Mice were group-housed in a 12 hour light/dark cycle. Food and water were provided *ad libitum*. Some Cre driver mice were crossed with the Cre-dependent tdTomato expressing reporter Ai14 (Madisen et al., 2010) or YFP expressing reporter Thy1-stop-YFP (Buffelli et al., 2003) for **Figure S1**.

Intravitreal injections and perfusions

Animals were anesthetized with ketamine/xylazine (100mg/kg ketamine, 10mg/kg xylazine). One drop of 0.5% proparacaine hydrochloride ophthalmic solution was applied as a topical anesthetic to the eye. A small incision was made by inserting a sharp 30 gauge needle to the depth of the bevel just below the limbus of the eye. A blunt 33 gauge needle attached to a Hamilton syringe was inserted to withdraw 2 μL of vitreous fluid. A second Hamilton syringe was used to inject 2 μL of virus. Needles were inserted between the len and the retina in order to minimize damage to either. Petroleum ophthalmic ointment was applied to the eye following surgery, and an analgesic was administered (ketoprofen for mice injected at the Allen Institute). Three weeks post-injection for Cre mice or post-tamoxifen induction for CreER mice, mice were deeply anesthetized with 5% isoflurane (at the Allen Institute) or 25 μL/10g Euthasol (Virbac; Fort Worth, TX; at Harvard) and intracardially perfused with 10 ml of saline (0.9% NaCl)

followed by 50 ml of freshly prepared 4% paraformaldehyde (PFA) at a flow rate of 9 ml/min. Brains were rapidly dissected and post-fixed in 4% PFA at room temperature for 3-6 hours and overnight at 4°C. rAAV injected eyes were dissected entirely from the eye cup and a cautery was used to mark the dorsal orientation on each eye, and were then post-fixed in 4% PFA for 30-60 min. Brains and eyes were rinsed briefly with PBS and stored in PBS with 0.1% sodium azide.

Immunohistochemistry

For whole mounts, retinas were first immunostained for GFP. Briefly, retinas were blocked in 0.3% Triton X-100 and 5% normal donkey serum in PBS on a shaker overnight at 4°C. The next day they were placed into primary antibody (chicken anti-GFP, Abcam, 1:1000 in 0.3% Triton X-100 and 5% normal donkey serum) and incubated for 1 week on a shaker at 4°C. Retinas were rinsed well in PBS, followed by incubation with secondary antibody (donkey anti-chicken Alexa Fluor 488, Jackson Immunoresearch, 1:500) on a shaker overnight at 4°C. Following immunohistochemistry, relaxing cuts were made and the retina was transferred to filter paper, mounted on glass slides using Fluoromount-G with DAPI (Southern Biotech), and coverslipped.

Retinas to be sectioned were immersed in 30% sucrose solution overnight at 4°C, embedded in TFM (General Data Healthcare, Inc), frozen to -80°C and sectioned at 20 μm in a cryostat (Leica 1850). For immunostaining, slides were rehydrated in PBS, then blocked in 0.3% Triton X-100 and 3% normal donkey serum in PBS for at least 30 minutes. Each slide was stained with anti-GFP antibody (chicken anti-GFP, Abcam, 1:1000) and one of the following additional primary antibodies: anti-Brn3a (mouse, Millipore, 1:500), anti-VAChT (guinea pig, Chemicon, 1:500-1000), anti-CART (rabbit, Phoenix Pharmaceuticals, 1:2000), anti-osteopontin (goat, R&D Systems, 1:1000), anti-RBPMS (guinea pig, PhosphoSolutions, 1:1250-2500), anti-melanopsin (rabbit, Thermo Scientific, 1:5000), anti-Foxp2 (rabbit, Abcam, 1:1500), anti-parvalbumin (rabbit, Swant, 1:5000-10,000) all diluted in 0.3% Triton X-100 and 3% normal donkey serum. Slides were incubated in primary antibodies overnight at 4°C, then washed in PBS and incubated in the following secondary antibodies for 90 minutes at room temperature: donkey anti-chicken Alexa Fluor 488 for GFP (donkey, Jackson Immunoresearch, 1:500), and anti-guinea pig, anti-rabbit or anti-mouse Alexa Fluor 555 (donkey, Jackson Immunoresearch, 1:500) for the other primary antibody detections. Slides were coverslipped using Fluoromount-G with DAPI (Southern Biotech).

Imaging

Brains from mice injected with tracer into one eye were prepared and imaged by serial two-photon tomography as previously described (Oh et al., 2014) using TissueCyte 1000 systems (TissueVision, Cambridge,MA) coupled with Mai Tai HP DeepSee lasers (Spectra Physics, Santa Clara, CA). Single optical plane images 75 μm below the tissue surface were acquired using 925 nm wavelength light through a Zeiss 320 water immersion objective (NA=1.0), with 250 mW light power at objective. In order to scan a full tissue section, individual tile images were acquired, and the entire stage was moved between each tile. Then, a vibratome cuts a 100 μm section and the imaging is repeated. Images are collected from 140 coronal sections covering the rostral-to-caudal extent of the brain, which takes ~18.5 h at an x,y resolution of ~0.35 μm per pixel.

Images were processed using the informatics data pipeline (IDP) set up and previously described in detail for the Allen Mouse Brain Connectivity Atlas (Oh et al., 2014;Kuan et al., 2015). Briefly, the two key algorithms are signal detection and image registration. The signal detection algorithm was applied to each image to segment positive fluorescent signals from background. The output is a full resolution mask that classifies each pixel as either signal or background. An isotropic 3-D summary of each brain is constructed by dividing each image into 10 □m X 10 □m grid voxels. Total signal is computed for each voxel by summing the number of signal-positive pixels in that voxel. The highly aligned nature from section to section allows for simply stacking the section images together to form a coherent reconstructed 3-D volume. Each image stack is then registered in a multi-step process using both global affine and local deformable registration to the 3-D Allen Common Coordinate Framework (CCF) as previously described (Oh et al., 2014;Kuan et al., 2015). Segmentation and registration results are combined to quantify signal for each voxel in the reference space and for each structure in the CCF ontology by combining voxels from the same structure.

Here, we used normalized projection volume as a measure of projection strength. Normalized projection volume is the sum of segmented pixels within a given brain structure divided by the sum of segmented pixels within the injection site. Because the injection site in these experiments was outside the imaged brain, we chose to normalize each target's value by the sum of segmented pixels within the optic chiasm. This signal should be more accurate as a value for injection size than what we could measure in the corresponding retinal whole mount as it includes all the RGC axons entering the brain from a particular experiment, and does not include other retinal cell types that might express Cre-dependent rAAV-EGFP. Connection weights were measured with pixel counts rather

than fluorescence intensity, because counts were previously determined to be more reliable (Oh et al., 2014). We chose to represent the weights in each target region by using volume (sum of detected pixels) and not density (sum of detected pixels / target structure volume). The scaling of results by injection size shows the proportion of axons going to each structure. In contrast, many anatomists are accustomed to categorizing projections by number rather than proportion of axons. As an illustration, imagine lines A and B that both project to area X. If line A has 5 axons at the chiasm and 5 in area X, Figure 10 shows a high value for the line A/area X box. If line B has 1000 axons at the chiasm and 50 in area X, the line B/area X box will have a low value. In contrast, conventional histology would categorize A as having a weak and B a strong projection to area X, because ratings are usually made on the basis of something closer to absolute density.

Unsupervised hierarchical clustering was done on the log-transformed normalized projection volumes using GENE-E or Morpheus software for algorithms and dendrogram visualization (http://www.broadinstitute.org/cancer/software/GENE-E/index.html). True negative values ("0s") were converted to the half minimum of the positive array elements before calculating the logarithm.

To subdivide LGd for analyses shown in **Figure 6**, sections from Kcng4-Cre (alpha RGCs), Cart-Tg1-Cre (ooDSGCs) and CTB-injected mice (in the opposite eye) were matched for rostral-caudal location and aligned to the average template brain used as the basis for drawing structures in the Allen Mouse CCF. The strongest projections (avoiding passing fibers, and above a set threshold) were pseudocolored by line. Borders were drawn as shown in **Figure 6** using the pseudocolored projection signal, as well as anatomical data derived from the average template brain.

References

Buffelli, M., Burgess, R.W., Feng, G., Lobe, C.G., Lichtman, J.W., and Sanes, J.R. (2003). Genetic evidence that relative synaptic efficacy biases the outcome of synaptic competition. *Nature* 424**,** 430-434.

Kuan, L., Li, Y., Lau, C., Feng, D., Bernard, A., Sunkin, S.M., Zeng, H., Dang, C., Hawrylycz, M., and Ng, L. (2015). Neuroinformatics of the Allen Mouse Brain Connectivity Atlas. *Methods* 73**,** 4-17.

Madisen, L., Zwingman, T.A., Sunkin, S.M., Oh, S.W., Zariwala, H.A., Gu, H., Ng, L.L., Palmiter, R.D., Hawrylycz, M.J., Jones, A.R., Lein, E.S., and Zeng, H. (2010). A robust and high-throughput Cre reporting and characterization system for the whole mouse brain. *Nat Neurosci* 13**,** 133-140.

Oh, S.W., Harris, J.A., Ng, L., Winslow, B., Cain, N., Mihalas, S., Wang, Q., Lau, C., Kuan, L., Henry, A.M., Mortrud, M.T., Ouellette, B., Nguyen, T.N., Sorensen, S.A., Slaughterbeck, C.R., Wakeman, W., Li, Y., Feng, D., Ho, A., Nicholas, E., Hirokawa, K.E., Bohn, P., Joines, K.M., Peng, H., Hawrylycz, M.J., Phillips, J.W., Hohmann, J.G., Wohnoutka, P., Gerfen, C.R., Koch, C., Bernard, A., Dang, C., Jones, A.R., and Zeng, H. (2014). A mesoscale connectome of the mouse brain. *Nature* 508**,** 207-214.